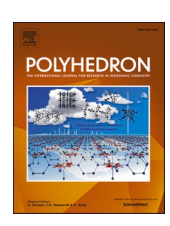


Contents lists available at ScienceDirect

# Polyhedron

journal homepage: www.elsevier.com/locate/poly





# Modular synthesis of diphosphoramidite ligands derived from 1,8,10,9-triazaboradecalin and their complexes with Ni, Pd, and Pt

Johnathan D. Culpepper<sup>1</sup>, Kyounghoon Lee<sup>2</sup>, Scott R. Daly<sup>\*</sup>

The University of Iowa. Department of Chemistry. E331 Chemistry Building, Iowa City. IA 52242, United States

#### ARTICLE INFO

Keywords:
Diphosphoramidite
Triaminoborane
Boron ligand
Pt-P coupling constant
P-M-P bite angle

#### ABSTRACT

Here we report a convenient synthesis of new diphosphoramidite ligands derived from 1,8,10,9-triazaboradecalin (TBD) and describe their complexes with group 10 metals. Treating the chlorinated and structurally characterized ligand precursor  $^{Cl}TBDPhos$  (L1) with four equivalents of HOR (R =  $C_3H_7$  or  $C_3HF_6$ ) in the presence of NEt<sub>3</sub> yielded the diphosphoramidite ligands <sup>iPrO</sup>TBDPhos (L2) and <sup>F-iPrO</sup>TBDPhos (L3) in good yields. L2 and L3 were used to prepare a variety of Ni, Pd, and Pt complexes with chloride and 1,2-benzenedithiolate ligands so their structures and spectroscopic properties could be compared to similar complexes with methoxy-substituted MeOTBDPhos such as (MeOTBDPhos)PdCl<sub>2</sub>, which is reported here for the first time. Single-crystal XRD studies on the (ROTBDPhos)PtCl<sub>2</sub> complexes revealed that increasing the size of alkoxy substituents from MeO to PrO to F-PrO decreases the P-M-P bite angle from 97.47(3)° in (MeOTBDPhos)PtCl<sub>2</sub> to 93.98(4)° in (F-iPrOTBDPhos)PtCl<sub>2</sub>. Similar changes were observed in the dithiolate complexes ( $^{iPrO}$ TBDPhos)Pt(S<sub>2</sub>C<sub>6</sub>H<sub>4</sub>) and ( $^{F\cdot iPrO}$ TBDPhos)Pt (S<sub>2</sub>C<sub>6</sub>H<sub>4</sub>), and the structural studies revealed longer Pt-P bond distances compared to the dichloride complexes that correlated to ca. 1000 Hz decrease in their <sup>195</sup>Pt-<sup>31</sup>P coupling constants. No significant changes were observed in the ligand bond distances in complexes containing the methoxy and isoproxy-substituted ligands, but complexes with fluorinated F-iPrOTBDPhos revealed subtle, but significant differences in their P-N, P-O, and B-N distances that reflect substituent-induced electronic changes in the ligand. Overall, this work establishes a more convenient synthetic entry into the chemistry of alkoxy-substituted TBDPhos ligands for ongoing studies with these and related transition metal complexes.

#### 1. Introduction

Phosphoramidites, trivalent phosphorus molecules that have two P-O and one P-N bond [1], have been used for applications such as the production of synthetic nucleic acid analogs [2–5], biological imaging dyes [6], and related biotechnological applications [7]. Phosphoramidites are also commonly used as ligands for coordination complexes and transition metal catalysts. These ligands are generally less  $\sigma$  donating than phosphines, but are better  $\pi\text{-acids}$  [8]. Much of the interest in phosphoramidites ligands stems from the outstanding utility of privileged chiral monophos variants in asymmetric catalysis, as discussed in numerous reviews and perspectives [9–21]. By comparison, there have been far fewer investigations focused on the development of chelating, diphosphoramidite ligands that contain two phosphoramidite

donors [22-28].

Our group recently reported the first example of a new diphosphoramidite ligand derived from 1,8,10,9-triazaboradecalin (TBD; Chart 1a) [29]. In general, we refer to diphosphorus ligands containing this triaminoborane as  $^{R}$ TBDPhos (where R is the substituent bound to phosphorus), and they are unique in that they can undergo *trans* H-X addition at the TBD backbone with Brønsted acids while bound to different transition metals (Chart 1b) [29–34]. Moreover, we have shown how the substituents attached to phosphorus are important for controlling this ligand-centered reactivity. For example, the ethylsubstituted diphosphine in ( $^{Et}$ TBDPhos)Pt(S<sub>2</sub>C<sub>6</sub>H<sub>4</sub>) is completely unreactive towards methanol and water whereas the methoxy-substituted diphosphoramidite in ( $^{MeO}$ TBDPhos)Pt(S<sub>2</sub>C<sub>6</sub>H<sub>4</sub>) undergoes immediate *trans* H-OR addition at the bridgehead *N*-B bond as soon as it

<sup>\*</sup> Corresponding author.

E-mail address: scott-daly@uiowa.edu (S.R. Daly).

<sup>&</sup>lt;sup>1</sup> Current address: Corning Incorporated, Corning, NY 14831, United States.

<sup>&</sup>lt;sup>2</sup> Current address: Gyeongsang National University, Department of Chemical Education and Research Institute of Natural Sciences, 501 Jinju-daero, Jinju 52828, Republic of Korea.

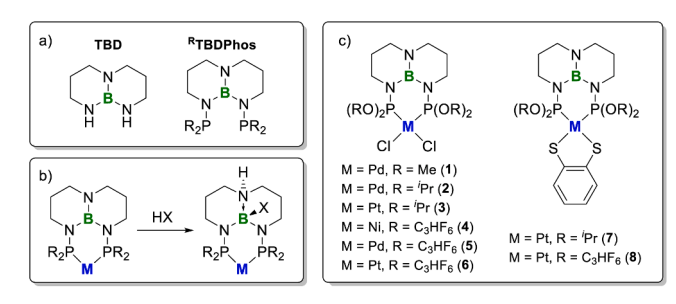


**Chart 1.** a) General structure of TBD and TBDPhos ligands. b) Reactivity of TBDPhos ligands with Brønsted acids (M = metal). c) Structures and numbering scheme of new complexes reported.

is contacted [29]. In general, we have found that  $^{\text{MeO}}$ TBDPhos is more reactive than phenyl- or alkyl-substituted TBDPhos ligands when bound to metals. Motivated by these observations, we set out to prepare other diphosphoramidite ligands like  $^{\text{MeO}}$ TBDPhos to investigate how different alkoxy substituents affect ligand-centered reactivity at the TBD backbone. Here we report a more convenient method to prepare TBD-derived phosphoramidite ligands, as illustrated with the synthesis of  $^{\text{iPrO}}$ TBDPhos and  $^{\text{F-iPrO}}$ TBDPhos (where F-iPrO = OC<sub>3</sub>HF<sub>6</sub>), and describe their complexes with Ni, Pd, and Pt.

#### 2. Experimental

#### 2.1. General considerations

Reactions were carried out under N2 or Ar atmospheres using glovebox or standard Schlenk techniques, unless stated otherwise. Glassware used for all reactions performed under inert conditions was dried in an oven at 150  $^{\circ}\text{C}$  for at least 2 h and allowed to cool under vacuum before use. Solvents used for F-iPrOTBDPhos (L3) chemistry were dried and distilled from sodium/benzophenone ketyl, degassed by freezepump thaw cycles and stored over 3 Å molecular sieves. All other solvents were dried and deoxygenated using a Pure Process Technologies Solvent Purification System and then stored over 3 Å molecular sieves under a N<sub>2</sub> atmosphere. 2-Propanol was refluxed over Mg turnings and distilled before use. 1,1,1,3,3,3-Hexafluoro-2-propanol (HFIP) was stored over 3 Å molecular sieves for at least three days before testing the water content. Karl Fisher titrations were performed on the HFIP reagent to test the water content, and it was found to be 15.6 ppm. Triethylamine was distilled and stored over KOH prior to use. All metal reagents such as (DME)NiCl<sub>2</sub>, (PhCN)<sub>2</sub>PdCl<sub>2</sub> and (COD)PtCl<sub>2</sub>, were purchased from commercial vendors, stored under either Ar or N2 glovebox atmosphere, and used without further purification. TBD and MeOTBDPhos were prepared following previously reported procedures [29,35–36].

 $^{1}H,~^{13}C,~^{11}B,~^{31}P,~$  and  $^{19}F$  NMR data were recorded on a Bruker AVANCE (500-MHz), a Bruker DRX (400-MHz), a Bruker AVANCEIII (400-MHz), or a Bruker AVANCE (300-MHz) NMR spectrometer. Chemical shifts are reported in  $\delta$  units in ppm referenced to residual solvent peaks ( $^{1}H$  and  $^{13}C$ ) or to 85%  $H_{3}PO_{4}$  ( $^{31}P;~\delta~0.0$  ppm), 0.05%  $C_{6}H_{5}CF_{3}$  in  $C_{6}D_{6}$  ( $^{19}F;~\delta~-62.9$ ), and  $BF_{3}\cdot Et_{2}O$  ( $^{11}B;~\delta~0.0$  ppm). Microanalysis data (CHN) were collected using an EAI CE-440 Elemental Analyzer at the University of Iowa's MATFab Facility. IR spectra were collected on a Thermo Scientific Nicolet iS5 using an attenuated total reflection (ATR) accessory.

## 2.2. ClTBDPhos (L1)

To a stirring solution of TBD (2.00 g, 14.4 mmol) and NEt $_3$  (2.90 g, 28.8 mmol) in Et $_2$ O (100 mL) was added PCl $_3$  (4.00 g, 29.1 mmol) dropwise at 0 °C. A white precipitate formed while the reaction was stirred overnight. The reaction was evaporated to dryness under vacuum and extracted with THF (100 mL  $\times$  3). The filtrate was evaporated to

dryness under vacuum, and the solid was dissolved in CH<sub>2</sub>Cl<sub>2</sub>. Colorless crystals were formed by cooling the solution to -30 °C. Yield: 3.47 g (70%). Anal. calcd for C<sub>6</sub>H<sub>12</sub>BC<sub>14</sub>N<sub>3</sub>P<sub>2</sub>: C, 21.15; H, 3.55; N, 12.33. Found: C, 20.77; H, 3.86; N, 12.65;  $^1$ H NMR (C<sub>6</sub>D<sub>6</sub>, 20 °C): δ 1.31 (4H, p, CH<sub>2</sub>-CH<sub>2</sub>-CH<sub>2</sub>), 2.14 (4H, t, NCH<sub>2</sub>), 3.06 (4H, m, NCH<sub>2</sub>).  $^{11}$ B NMR (C<sub>6</sub>D<sub>6</sub>, 20 °C): δ 22.8 (br s, FWHM = 150 Hz).  $^{13}$ C{ $^1$ H} NMR (C<sub>6</sub>D<sub>6</sub>, 20 °C): δ 26.4 (s, CH<sub>2</sub>-CH<sub>2</sub>-CH<sub>2</sub>), 42.5 (t, NCH<sub>2</sub>, J=3 Hz), 47.0 (s, NCH<sub>2</sub>).  $^{31}$ P{ $^1$ H} NMR (C<sub>6</sub>D<sub>6</sub>, 20 °C): δ 164.5 (s). MS (EI) [fragment ion, relative abundance]: m/z 340 [M, 18], 303 [M–Cl, 100], 267 [M–2Cl, 37], 232 [M–3Cl, 22]. IR (ATR, cm $^{-1}$ ): 2961 w, 2938 w, 2879 w, 2855 w, 2832 w, 1545 m, 1523 s, 1463 m, 1451 vw, 1439 s, 1370 s, 1345 s, 1321 s, 1287 s, 1267 vs, 1209 vs, 1153 s, 1116 m, 1103 s, 1094 s, 1056 m, 1033 vs, 1004 m, 982 s, 901 m, 877 s, 820 s, 790 vw, 763 s, 715 vw, 698 vw, 690 vw, 673 w, 658 m, 640 vs, 627 vs, 612 vs.

## 2.3. iPrOTBDPhos (L2)

To stirring solution of <sup>Cl</sup>TBDPhos (1.52 g, 4.47 mmol) and NEt<sub>3</sub> (1.81 g, 17.9 mmol) in CH<sub>2</sub>Cl<sub>2</sub> (200 mL) was added 2-propanol (1.81 g, 17.9 mmol) dropwise at 0 °C. A white precipitate formed while the reaction stirred overnight. The mixture was evaporated to dryness under vacuum, extracted with THF (100 mL  $\times$  3), and filtered. The filtrate was concentrated to yield a clear oil. Yield: 1.44 g (74%). <sup>1</sup>H NMR (CDCl<sub>3</sub>, 20 °C):  $\delta$  1.20 (24H, dd, OCH(CH<sub>3</sub>)<sub>2</sub>, J = 15.9 Hz, J = 6.2 Hz), 1.74 (4H, m,  $CH_2$ - $CH_2$ - $CH_2$ ), 2.83 (4H, t,  $NCH_2$ , J = 6.3 Hz), 3.12 (4H, m,  $NCH_2$ ), 4.16 (4H, m, OCH(CH<sub>3</sub>)<sub>2</sub>). <sup>11</sup>B NMR (CDCl<sub>3</sub>, 20 °C):  $\delta$  24.8 (br s, FWHM = 440 Hz).  ${}^{13}\text{C}\{\overline{}^{1}\text{H}\}$  NMR (CDCl<sub>3</sub>, 20 °C):  $\delta$  24.4 (t, OCH(CH<sub>3</sub>)<sub>2</sub>, J = 2.7 Hz), 24.5 (t, OCH(CH<sub>3</sub>)<sub>2</sub>, J = 2.7 Hz), 27.7 (s, CH<sub>2</sub>-CH<sub>2</sub>-CH<sub>2</sub>), 36.8 (s, NCH<sub>2</sub>), 48.5 (s, NCH<sub>2</sub>), 66.7 (t, OCH(CH<sub>3</sub>)<sub>2</sub>, J = 11.7 Hz). <sup>31</sup>P{<sup>1</sup>H} NMR  $(CDCl_3, 20 \, ^{\circ}C)$ :  $\delta \, \overline{139.1}$  (s). IR (ATR, cm<sup>-1</sup>): 2970 w, 2930 w, 2860 w, 1710 vw, 1510 w, 1460 w, 1440 w, 1380 m, 1320 w, 1300 m, 1210 w, 1170 m, 1060 w, 1030 w, 982 m, 947 vs, 880 w, 849 s, 812 m, 760 m, 724 s, 650 w, 603 w.

## 2.4. F-iPrOTBDPhos (L3)

To stirring solution of <sup>Cl</sup>TBDPhos (1.2 g, 3.5 mmol) and NEt<sub>3</sub> (1.43 g, 14.1 mmol) in CH<sub>2</sub>Cl<sub>2</sub> (200 mL) was added 1,1,1,3,3,3-hexafluoro-2propanol (2.37 g, 14.1 mmol) dropwise at 0  $^{\circ}$ C. A white precipitate formed while the reaction was stirred overnight. The mixture was evaporated to dryness under vacuum, extracted with THF (200 mL), and filtered. The filtrate was evaporated to dryness under vacuum, dissolved in CH<sub>2</sub>Cl<sub>2</sub> filtered, and then concentrated. Colorless crystals were formed at -30 °C, washed with cold pentane, and evaporated to dryness under vacuum. Yield: 2.72 g (89%). Anal. Calcd for C<sub>18</sub>H<sub>16</sub>BF<sub>24</sub>N<sub>3</sub>O<sub>4</sub>P<sub>2</sub>: C, 24.93; H, 1.86; N, 4.85. Found: C, 25.13; H, 1.94; N, 4.72. <sup>1</sup>H NMR (CDCl<sub>3</sub>, 20 °C):  $\delta$  1.85 (4H, m, CH<sub>2</sub>-CH<sub>2</sub>-CH<sub>2</sub>), 2.93 (4H, t, NCH<sub>2</sub>, J = 6.3 Hz), 3.25 (4H, m, NCH<sub>2</sub>), 4.58 (4H, septet, OCH(CF<sub>3</sub>)<sub>2</sub>, J = 5.1 Hz). <sup>11</sup>B NMR (CDCl<sub>3</sub>, 20 °C):  $\delta$  24.2 (br s, FWHM = 300 Hz). <sup>13</sup>C{<sup>1</sup>H} NMR  $(CDCl_3, 20 \,^{\circ}C)$ :  $\delta$  26.6 (s,  $CH_2$ - $CH_2$ - $CH_2$ ), 38.1 (s,  $NCH_2$ ), 47.7 (s,  $NCH_2$ ), 70.7 (m, OCH (CF<sub>3</sub>)<sub>2</sub>), 121.1 (q, OCH (CF<sub>3</sub>)<sub>2</sub>, J = 284 Hz). <sup>19</sup>F NMR (CDCl<sub>3</sub>, 20 °C):  $\delta$  –74.3 (m), –74.5 (m).  $\overline{^{31}}$ P{<sup>1</sup>H} NMR (CDCl<sub>3</sub>, 20 °C):  $\delta$ 152.1 (s). IR (ATR, cm<sup>-1</sup>): 2962 vw, 2936 vw, 2898 vw, 2870 vw, 2602 vw, 2497 vw, 2004 vw, 1548 w, 1530 w, 1475 w, 1445 w, 1369 m, 1328 w, 1292 m, 1267 m, 1216 s, 1191 s, 1095 s, 1037 m, 1010 m, 983 m, 900 m, 869 s, 806 s, 782 s, 722 w, 685 s, 649 m.

## 2.5. (MeOTBDPhos)PdCl<sub>2</sub> (1)

To a stirring solution of  $^{\text{MeO}}$ TBDPhos (0.50 g, 1.6 mmol) in CH<sub>2</sub>Cl<sub>2</sub> (30 mL) was added a solution of (PhCN)<sub>2</sub>PdCl<sub>2</sub> (0.594 g, 1.55 mmol) in CH<sub>2</sub>Cl<sub>2</sub> (10 mL). The reaction mixture was stirred overnight, then filtered and concentrated to  $\sim$  3 mL. Crystals were grown by vapor diffusion with Et<sub>2</sub>O at RT and isolated by decanting the mother liquor and evaporating them to dryness under vacuum. Yield: 0.65 g (84%). Anal. Calcd for C<sub>10</sub>H<sub>24</sub>BCl<sub>2</sub>N<sub>3</sub>O<sub>4</sub>P<sub>2</sub>Pd•(C<sub>4</sub>H<sub>10</sub>O)<sub>0.25</sub>: C, 25.46; H, 5.15; N,

8.10. Found: C, 25.73; H, 4.73; N, 8.64.  $^{1}$ H NMR (CDCl<sub>3</sub>, 20  $^{\circ}$ C):  $\delta$  1.84 (4H, quint, CH<sub>2</sub>-CH<sub>2</sub>-CH<sub>2</sub>), 2.94 (4H, t, NCH<sub>2</sub>), 3.25 (4H, m, NCH<sub>2</sub>), 3.92 (12H, OCH<sub>3</sub>).  $^{11}$ B NMR (CDCl<sub>3</sub>, 20  $^{\circ}$ C):  $\delta$  22.8 (br s, FWHM = 310 Hz).  $^{31}$ P{ $^{1}$ H} NMR (CDCl<sub>3</sub>, 20  $^{\circ}$ C):  $\delta$  96.2. IR (ATR, cm $^{-1}$ ): 3004 vw, 2935 w, 2905 w, 2879 w, 2852 w, 2154 vw, 1976 vw, 1511 m, 1452 m, 1389 m, 1363 m, 1322 m, 1284 s, 1208 m, 1168 m, 1113 w, 1086 m, 1004 vs, 920 s, 888 w, 810 vs, 772 s, 622 s.

## 2.6. (iPrOTBDPhos)PdCl<sub>2</sub> (2)

To stirring solution of (PhCN)<sub>2</sub>PdCl<sub>2</sub> (0.276 g, 0.720 mmol) in CH<sub>2</sub>Cl<sub>2</sub> (10 mL) was added L2 (0.313 g, 0.720 mmol) dissolved in CH<sub>2</sub>Cl<sub>2</sub> (10 mL) at room temperature. The reaction mixture changed color from dark-reddish orange to green as it was stirred overnight. The mixture was evaporated to dryness under vacuum, and blocky green XRD quality crystals were grown by vapor diffusion of pentane into a concentrated toluene solution. Yield: 0.285 g (65%). <sup>1</sup>H NMR (CDCl<sub>3</sub>, 20 °C):  $\delta$  1.35 (24H, dd, OCH(CH<sub>3</sub>)<sub>2</sub>, J = 6.1 Hz), 1.81 (4H, m, CH<sub>2</sub>-CH<sub>2</sub>- $CH_2$ ), 2.91 (4H, t,  $NCH_2$ ,  $J = 6.\overline{1}$  Hz), 3.27 (4H, m,  $NCH_2$ ), 5.33 (4H, m, OCH(CH<sub>3</sub>)<sub>2</sub>). <sup>11</sup>B NMR (CDCl<sub>3</sub>, 20 °C):  $\delta$  22.0 (br s, FWHM = 380 Hz).  $^{13}\text{C}\{^{1}\text{H}\}$  NMR (CDCl<sub>3</sub>, 20 °C):  $\delta$  23.8 (m, OCH(CH<sub>3</sub>)<sub>2</sub>), 25.6 (s, CH<sub>2</sub>-CH<sub>2</sub>-CH<sub>2</sub>), 41.2 (s, NCH<sub>2</sub>), 48.6 (s, NCH<sub>2</sub>), 73.8 (s, OCH(CH<sub>3</sub>)<sub>2</sub>), <sup>31</sup>P{<sup>1</sup>H} NMR (CDCl<sub>3</sub>, 20 °C):  $\delta$  87.6 (s). IR (ATR, cm<sup>-1</sup>): 2967 w, 2931 w, 2884 w, 1508 m, 1465 w, 1444 w, 1368 m, 1354 w, 1354 w, 1321 m, 1305 m, 1287 s, 1213 s, 1173 m, 1142 m, 1095 s, 1066 w, 1028 s, 960 vs, 923 vs, 884 s, 834 s, 798 s, 757 s, 731 s, 652 m, 633 s, 613 s.

## 2.7. (iPrOTBDPhos)PtCl<sub>2</sub> (3)

To a stirring solution of (COD)PtCl<sub>2</sub> (0.450 g, 1.20 mmol) in CH<sub>2</sub>Cl<sub>2</sub> (5 mL) was added a solution of L2 (0.522 g, 1.20 mmol) in  $CH_2Cl_2$  (15 mL). The colorless reaction mixture was stirred overnight and evaporated to dryness. The residue was dissolved in THF and crystallized by vapor diffusion with pentane. Yield: 0.505 g (52%). Crystals can also be grown by vapor diffusion with toluene and pentane. Anal. Calcd for C<sub>18</sub>H<sub>40</sub>BCl<sub>2</sub>N<sub>3</sub>O<sub>4</sub>P<sub>2</sub>Pt: C, 30.83; H, 5.75; N, 5.99. Found: C, 30.47; H, 5.54; N, 5.44. <sup>1</sup>H NMR (CDCl<sub>3</sub>, 20 °C):  $\delta$  1.34 (24H, dd, OCH(C<u>H</u><sub>3</sub>)<sub>2</sub>, J = 23.3 Hz, J = 6.2 Hz), 1.84 (4H, m, CH<sub>2</sub>-CH<sub>2</sub>-CH<sub>2</sub>), 2.91 (4H, t, NCH<sub>2</sub>, J =6.0 Hz), 3.25 (4H, m, NCH<sub>2</sub>), 5.25 (4H, m, OCH(CH<sub>3</sub>)<sub>2</sub>). <sup>11</sup>B NMR (CDCl<sub>3</sub>, 20 °C):  $\delta$  22.3, (br s FWHM = 350 Hz).  $^{13}\overline{\text{C}}\{^{1}\text{H}\}$  NMR (CDCl<sub>3</sub>, 20 °C):  $\delta$  23.7 (m, OCH(CH<sub>3</sub>)<sub>2</sub>), 25.5 (s, CH<sub>2</sub>-CH<sub>2</sub>-CH<sub>2</sub>), 41.2 (s, NCH<sub>2</sub>), 48.7 (s, NCH<sub>2</sub>), 73.01 (s,  $\overline{\text{OCH}(\text{CH}_3)_2}$ ).  $^{31}\text{P}\{^1\text{H}\}$  NMR (CDCl<sub>3</sub>, 20 °C): (s)  $\delta$ 60.7 (s with doublet satellites,  ${}^{1}J_{PtP} = 4882 \text{ Hz}$ ). IR (ATR, cm $^{-1}$ ): 2970 w, 2920 w, 2880 w, 2850 w, 1530 w, 1510 w, 1460 vw, 1450 w, 1390 w, 1370 w, 1350 w, 1320 w, 1300 vw, 1290 w, 1210 w, 1170 w, 1140 w, 1090 w, 1060 vw, 1030 w, 960 s, 924 m, 883 m, 835 w, 799 w, 740 w, 658 w, 626 m.

## 2.8. (F-iPrOTBDPhos)NiCl<sub>2</sub> (4)

To a stirring solution of (DME)NiCl<sub>2</sub> (0.177 g, 0.461 mmol) in CH<sub>2</sub>Cl<sub>2</sub> (10 mL) was added a solution of L3 (0.400 g, 0.461 mmol) in CH<sub>2</sub>Cl<sub>2</sub> (10 mL). The yellow reaction mixture turned orange as it was stirred overnight. The mixture was filtered and concentrated to about  $\sim$  3 mL. Colored crystals were grown by cooling the solution to -30 °C. Yield: 0.313 g (68%). Anal. Calcd for  $C_{18}H_{16}BC_{12}F_{24}N_3O_4P_2Ni$ : C, 21.69; H, 1.62; N, 4.22. Found: C, 21.96; H, 1.64; N, 4.12. <sup>1</sup>H NMR (CDCl<sub>3</sub>, 20 °C):  $\delta$  1.87 (4H, s, CH<sub>2</sub>-CH<sub>2</sub>-CH<sub>2</sub>),  $\delta$  2.97 (4H, s, NCH<sub>2</sub>),  $\delta$  3.37 (4H, s, NCH<sub>2</sub>), 6.19 (4H, s, OCH(CF<sub>3</sub>)<sub>2</sub>). <sup>11</sup>B NMR (CDCl<sub>3</sub>, 20 °C):  $\delta$  21.4 (br s, FWHM = 400 Hz).  $^{13}$ C{ $^{1}$ H} NMR (CDCl<sub>3</sub>, 20  $^{\circ}$ C):  $\delta$  25.0 (s, CH<sub>2</sub>-CH<sub>2</sub>-CH<sub>2</sub>), 42.3 (s, NCH<sub>2</sub>), 48.1 (s, NCH<sub>2</sub>), 73.4 (s, OCH(CF<sub>3</sub>)<sub>2</sub>), 119.3 (d, OCH(CF<sub>3</sub>)<sub>2</sub>), J =77 Hz), 121.5 (d, OCH(CF<sub>3</sub>)<sub>2</sub>,  $J = \overline{77}$  Hz). <sup>31</sup>P{<sup>1</sup>H} NMR (CDCl<sub>3</sub>, 20 °C): (s)  $\delta$  98.1 (s).  $^{19}\text{F}$  NMR (CDCl3, 20 °C):  $\delta$  -72.9 (s), -74.2 (s). IR (ATR, cm<sup>-1</sup>): 2956 w, 2905 vw, 2871 vw, 2158 w, 2020 w, 1977 w, 1548 w, 1529 m, 1478 w, 1457 w, 1443 vw, 1399 w, 1378 m, 1373 m, 1333 m, 1289 s, 1260 m, 1224 s, 1192 vs, 1091 vs, 1035 s, 933 m, 896 s, 864 s,

832 s, 796 s, 734 s, 686 vs, 631 s.

## 2.9. (F-iPrOTBDPhos)PdCl<sub>2</sub> (5)

To a stirring solution of (PhCN)<sub>2</sub>PdCl<sub>2</sub> (0.177 g, 0.461 mmol) in CH<sub>2</sub>Cl<sub>2</sub> (10 mL) was added a solution of **L3** (0.400 g, 0.461 mmol) in CH<sub>2</sub>Cl<sub>2</sub> (10 mL). The reaction mixture turned golden brown while being stirred overnight. The mixture was filtered, concentrated to ~ 3 mL, and cooled to ~30 °C to afford brown crystals. Yield: 0.270 g (56%). Anal. Calcd for C<sub>18</sub>H<sub>16</sub>BC<sub>12</sub>F<sub>24</sub>N<sub>3</sub>O<sub>4</sub>P<sub>2</sub>Pd: C, 20.7; H, 1.54; N, 4.02. Found: C, 21.5; H, 1.84; N, 3.66. <sup>1</sup>H NMR (CDCl<sub>3</sub>, 20 °C):  $\delta$  1.94 (4H, m, CH<sub>2</sub>-CH<sub>2</sub>-CH<sub>2</sub>), 3.03 (4H, t, NCH<sub>2</sub>, J = 6.1 Hz), 3.48 (4H, m, NCH<sub>2</sub>), 6.26 (4H, m, OCH(CF<sub>3</sub>)<sub>2</sub>). <sup>11</sup>B NMR (CDCl<sub>3</sub>, 20 °C):  $\delta$  21.6 (br s, FWHM = 400 Hz). <sup>31</sup>P (<sup>1</sup>H) NMR (CDCl<sub>3</sub>, 20 °C): (s)  $\delta$  96.5 (s). <sup>19</sup>F NMR (CDCl<sub>3</sub>, 20 °C):  $\delta$  ~73.0 (s), ~74.0 (s). IR (ATR, cm<sup>-1</sup>): 2962 w, 2905 vw, 2872 vw, 2010 vw, 1548 w, 1529 m, 1476 vw, 1455 vw, 1435 vw, 1396 w, 1358 w, 1333 w, 1295 m, 1259 s, 1195 s, 1086 vs, 1032 vs, 941 s, 898 m, 874 s, 843 s, 795 s, 732 m, 687 vs, 643 m, 623 m.

#### 2.10. (F-iPrOTBDPhos)PtCl<sub>2</sub> (6)

To a stirring solution of (COD)PtCl $_2$  (0.086 g, 0.231 mmol) in CH $_2$ Cl $_2$  (5 mL) was added a solution of L3 (0.200 g, 0.231 mmol) in CH $_2$ Cl $_2$  (10 mL). The colorless reaction mixture was stirred overnight. The mixture was filtered and concentrated to about  $\sim 3$  mL. Colorless crystals were grown by cooling the solution to  $-30\,^{\circ}$ C. Yield: 0.202 g (77%). Anal. Calcd for C18H16BCl2F24N3O4P2Pt: C, 19.08; H, 1.42; N, 3.71. Found: C, 20.24; H, 1.64; N, 3.17.  $^{1}$ H NMR (CDCl $_3$ , 20  $^{\circ}$ C):  $\delta$  1.94 (4H, m, CH $_2$ -CH $_2$ -CH $_2$ ), 3.02 (4H, t, NCH $_2$ , J=6.1 Hz), 3.45 (4H, m, NCH $_2$ ), 6.11 (4H, m, OCH(CF $_3$ ) $_2$ ).  $^{11}$ B NMR (CDCl $_3$ , 20  $^{\circ}$ C):  $\delta$  21.8 (br s, FWHM = 250 Hz).  $^{19}$ F NMR (CDCl $_3$ , 20  $^{\circ}$ C):  $\delta$  -73.9 (s).  $^{31}$ P{ $^{1}$ H} NMR (CDCl $_3$ , 20  $^{\circ}$ C): (s)  $\delta$  69.6 (s with doublet satellites,  $^{1}$ J $_{PtP}=4895$  Hz). IR (ATR, cm $^{-1}$ ): 2956 w, 2905 vw, 2871 vw, 2005 vw, 1547 w, 1527 m, 1477 w, 1456 w, 1434 w, 1397 m, 1362 m, 1333 m,1295 s, 1259 m, 1225 s, 1193 s, 1090 s, 1035 s, 942 m, 897 s, 874 s, 846 s, 802 m, 733 m, 687 s, 654 m, 626 m.

## 2.11. ( $^{iPrO}TBDPhos$ ) $Pt(S_2C_6H_4)$ (7)

1,2-Benzenedithiol (0.071 g, 0.498 mmol) was added to a stirring solution of **3** (0.20 g, 0.249 mmol) with excess NEt<sub>3</sub> (2.18 g, 21.5 mmol) in CH<sub>2</sub>Cl<sub>2</sub> (200 mL). The reaction was evaporated to dryness under vacuum and extracted with THF (100 mL  $\times$  3). The filtrate was evaporated to dryness under vacuum, dissolved in toluene, and crystallized by vapor diffusion with pentane. Yield: 0.156 g (81%). Anal. Calcd for C<sub>24</sub>H<sub>44</sub>BN<sub>3</sub>O<sub>4</sub>P<sub>2</sub>PtS<sub>2</sub>: C, 37.41; H, 5.76; N, 5.45. Found: C, 37.99; H, 5.81; N, 5.38. <sup>1</sup>H NMR (CDCl<sub>3</sub>, 20 °C):  $\delta$  1.24 (d, OCH(CH<sub>3</sub>)<sub>2</sub>, 12H, J = 6.0 Hz), 1.39 (d, OCH(CH<sub>3</sub>)<sub>2</sub>, 12H, J = 6.0 Hz), 1.85 (m, CH<sub>2</sub>-CH<sub>2</sub>-CH<sub>2</sub>, 4H), 2.94 (t, NCH<sub>2</sub>, 4H), 3.32 (m, NCH<sub>2</sub>, 4H), 5.18 (m, OCH(CH<sub>3</sub>)<sub>2</sub>, 4H), 6.81 (m, Ar, 2H), 7.59 (m, Ar, 2H). <sup>11</sup>B NMR (CDCl<sub>3</sub>, 20 °C):  $\delta$  22.5 (br s, FWHM = 480 Hz).  ${}^{31}P\{^{1}H\}$  NMR (CDCl<sub>3</sub>, 20 °C): (s)  $\delta$  89.7 (s with doublet satellites,  ${}^{1}J_{PtP} = 3895 \text{ Hz}$ ). IR (ATR, cm $^{-1}$ ): 2970 w, 2930 w, 2880 w, 2850 w, 1730 vw, 1510 w, 1470 w, 1450 w, 1380 w, 1370 w, 1350 w, 1320 w, 1290 w, 1210 w, 1170 w, 1140 w, 1090 w, 1060 vw, 960 s, 924 m, 882 m, 835 w, 798 w, 778 w, 740 w 658 w, 625 w.

# 2.12. $(^{F-iPrO}TBDPhos)Pt(S_2C_6H_4)$ (8)

To a stirring solution of **6** (0.20 g, 0.177 mmol) with excess NEt<sub>3</sub> (2.18 g, 21.5 mmol) in CH<sub>2</sub>Cl<sub>2</sub> (30 mL) was added 1,2-benzenedithiol (0.025 g, 0.0.177 mmol). The reaction mixture was stirred overnight, evaporated to dryness under vacuum, and then extracted with THF. The extract was evaporated to dryness under vacuum, dissolved in CH<sub>2</sub>Cl<sub>2</sub>, and crystallized by cooling to  $-30\,^{\circ}\text{C}$ . Yield: 0.0842 g (40%). Anal. Calcd for C<sub>24</sub>H<sub>20</sub>BF<sub>24</sub>N<sub>3</sub>O<sub>4</sub>P<sub>2</sub>PtS<sub>2</sub>: C, 23.97; H, 1.68; N, 3.49. Found: C, 25.06; H, 1.96; N, 3.12.  $^{1}\text{H}$  NMR (CDCl<sub>3</sub>, 20  $^{\circ}\text{C}$ ):  $\delta$  1.96 (m, CH<sub>2</sub>-CH<sub>2</sub>-CH<sub>2</sub>, 4H),

Crystallographic data for CTBDPhos (L1), (McCTBDPhos)PdCl<sub>2</sub> (1), (HPOTBDPhos)PdCl<sub>2</sub> (2), (HPOTBDPhos)PdCl<sub>2</sub> (3), (F-IPOTBDPhos)PtCl<sub>2</sub> (6), (HPOTBDPhos)PtCl<sub>2</sub> (7), (HPOTBDPhos)PtCl<sub>2</sub> (1), (HP

or yamingrapine data rot	1001 (41), (	calystanographic data for the first most acid (1), ( ) the first most acid (2), ( ) the first most for (0), (	1103)1 doi2 (2), ( 1101)		1 DE 1103)1 (912 (91), ( 1 DE 1103)1 ((9296114) (71), and (	(020614) (1), and (	1551 1657 (62%) (9).
	L1	1	2	3	9	7	8
Formula	C <sub>6</sub> H <sub>12</sub> BCl <sub>4</sub> N3P2	C <sub>10</sub> H <sub>24</sub> BCl <sub>2</sub> N <sub>3</sub> O <sub>4</sub> P <sub>2</sub> Pd	C <sub>18</sub> H <sub>40</sub> BCl <sub>2</sub> N <sub>3</sub> O <sub>4</sub> P <sub>2</sub> Pd	C <sub>18</sub> H <sub>40</sub> BCl <sub>2</sub> N <sub>3</sub> O <sub>4</sub> P <sub>2</sub> Pt	C <sub>18</sub> H <sub>16</sub> BCl <sub>2</sub> F <sub>24</sub> N <sub>3</sub> O <sub>4</sub> P <sub>2</sub> Pt	C <sub>24</sub> H <sub>44</sub> BN <sub>3</sub> O <sub>4</sub> P <sub>2</sub> PtS <sub>2</sub>	C <sub>24</sub> H <sub>20</sub> BF <sub>24</sub> N <sub>3</sub> O <sub>4</sub> P <sub>2</sub> PtS <sub>2•</sub> CH <sub>2</sub> Cl <sub>2</sub>
FW (g $\text{mol}^{-1}$ )	340.74	500.37	612.61	701.27	1133.08	770.58	1287.31
Identifier	Dal18_5	Dal19_26	Dal21_58	Dal19_64	Dal20_15	Dal20_24	Dal21_17
crystal system	monoclinic	orthorhombic	monoclinic	monoclinic	monoclinic	monoclinic	orthorhombic
space group	C2/c	Pbcn	$P2_1/n$	$P2_1/n$	$P2_1/n$	$P2_1/n$	$P2_12_12_1$
a (Å)	9.6418(10)	14.9049(15)	11.5705(10)	9.3742(9)	16.4635(16)	10.8432(11)	11.0362(11)
b (Å)	8.7977(9)	11.3140(11)	11.5422(11)	16.4915(16)	17.8567(18)	21.148(2)	18.0727(18)
c (Å)	16.1399(16)	11.2987(11)	20.859(2)	17.4485(17)	24.108(2)	13.8435(14)	20.645(2)
α (deg)	06	06	06	06	06	06	06
β (deg)	96.531	06	102.265(5)	93.268(5)	106.076(5)	102.806(5)	06
γ (deg)	06	06	06	06	06	06	06
volume $(\mathring{A}^3)$	1360.2(2)	1905.3(3)	2722.1(5)	2693.1(5)	6810.2(11)	3095.5(5)	4117.7(7)
Z	4	4	4	4	8	4	4
$ ho_{ m calc}$ (g cm $^{-3}$ )	1.664	1.744	1.495	1.730	2.210	1.653	2.077
$\mu \text{ (mm}^{-1})$	1.080	1.440	1.023	5.556	4.537	4.805	3.864
F(000)	889	1008	1264	1392	4320	1544	2480
$\theta$ range (deg)	3.144/26.371	2.733/26.460	1.998/28.312	2.411/27.247	1.343/26.422	2.153/26.396	2.092/27.906
R(int)	0.208	0.0613	0.0295	0.0514	0.0650	0.0324	0.0456
data/restraints/parameters	1379/0/75	1968/0/109	6743/30/310	5988/0/288	13988/0/1000	6342/0/342	9791/151/642
GOF	1.090	1.046	1.087	1.016	1.035	1.058	1.064
$ m R_1 \ [I>2\sigma(I)]^a$	0.0216	0.0274	0.0225	0.0281	0.0295	0.0134	0.0222
$wR_2$ (all data) <sup>b</sup>	0.0540	0.0606	0.0534	0.0662	0.0576	0.0316	0.0510
Largest Peak/Hole (e· $Å^{-3}$ )	0.222/-0.245	0.423/-0.408	0.733/-0.742	1.032/-0.849	0.709/-0.611	0.441/-0.767	0.929/-0.681
Temp (K)	190(2)	150(2)	150(2)	150(2)	150(2)	100(2)	150(2)

 $= \sum |F_o| - |F_c| |/| \sum |F_o| \text{ for reflections with } F_o^2 > 2 \text{ } \sigma(F_o^2).$   $t_2 = [\sum w(F_o^2 - F_c^2)^2 / \sum (F_o^2)^2]^{1/2} \text{ for all reflections.}$ 

3.03 (t, NCH $_2$ , 4H), 3.52 (m, NCH $_2$ , 4H),  $\delta\,6.19$  (m, OCH(CF $_3$ ) $_2$ , 4H), 7.01 (m, Ar, 2H), 7.70 (m, Ar, 2H).  $^{11}B$  NMR (CDCl $_3$ , 20  $^{\circ}$ C):  $\delta\,$ 22.2 (br s, FWHM = 340 Hz).  $^{31}P\{^1H\}$  NMR (CDCl $_3$ , 20  $^{\circ}$ C): (s)  $\delta\,$  102.6 (s with doublet satellites,  $^1J_{PtP}=3852$  Hz).  $^{19}F$  NMR (CDCl $_3$ , 20  $^{\circ}$ C):  $\delta\,$  -72.6 (s), -72.7 (s). IR (ATR, cm $^{-1}$ ): 2955 vw, 2927 w, 2865 vw, 2160 vw, 2020 vw, 1970 vw, 1559 vw, 1537 vw, 1522 m, 1476 w, 1451 w, 1422 w, 1399 w,1360 m, 1331 m, 1289 m, 1222 s,1192 s, 10932 s, 1033 s, 940 m, 894 m, 863 s, 825 s, 742 s, 686 s, 643 m.

#### 2.13. Single-crystal XRD studies

Single crystals obtained from CH<sub>2</sub>Cl<sub>2</sub>/Et<sub>2</sub>O (1), toluene/pentane (2, 3, and 7), or CH<sub>2</sub>Cl<sub>2</sub> (L1, 6, and 8) were mounted on a MiTeGen micromount using ParatoneN oil in air. The data collection, structural solution, and refinement were carried out as reported previously. The data were corrected for absorption using redundant reflections and the SADABS program [37]. The structures were solved with direct methods (SHELXS) or intrinsic phasing (SHELXT) [38], and non-hydrogen atoms were confirmed with least-square methods (SHELXL) [39]. The final refinement included anisotropic temperature factors for all nonhydrogen atoms. The positions of the hydrogen atoms were idealized and allowed to ride on the attached carbon atoms. HKL reflections with error/esd values  $\pm 10$  were omitted from the models. A set of CH<sub>3</sub> groups in the structure of 2 and a set of CF<sub>3</sub> groups in the structure of 8 were disordered, which required restraints on the C-C and C-F bond distances and anisotropic parameters to obtain satisfactory models. The disordered C-CH<sub>3</sub> distances in 2 and were constrained to be equal with an esd of 0.005 Å, whereas the disordered C-CF<sub>3</sub>, C-F, and F•••F distances in 8 were each constrained to be equal with an esd of 0.01 Å. SIMU and ISOR commands were used to obtain satisfactory ellipsoids and prevent nonpositive-definites for the disordered atoms in both structures. Structure solution and refinement were carried out using Olex2 [40], and publication figures were generated using Mercury CSD 3.10 [41]. Data collection and refinement details are compiled in Table 1.

#### 3. Results and discussion

## 3.1. Ligand synthesis

In our previous report [29], we described how MeOTBDPhos was prepared by treating TBD with two equivalents of ClP(OMe)2 in the presence of base, as shown in Scheme 1. Given that the synthesis and purification of ClP(OR)<sub>2</sub> precursors can be challenging due to formation of other Cl<sub>n</sub>P(OR)<sub>3-n</sub> products, we sought a more convenient synthetic method to prepare alkoxy-substituted TBDPhos derivatives. It has been shown that diphosphinite ligands with the general formula (RO)<sub>2</sub>P  $(CH_2)_n P(OR)_2$  (where R = alkyl or aryl) can be prepared by treating the corresponding Cl<sub>2</sub>P(CH<sub>2</sub>)<sub>n</sub>PCl<sub>2</sub> precursor with alcohols in the presence of base [42–45]. To determine the feasibility of this route for preparing diphosphoramidite ligands with TBD, we first prepared <sup>Cl</sup>TBDPhos (L1) by addition of NEt3 to a colorless solution of TBD in Et2O, followed by dropwise additions of PCl3 at 0 °C. Crystalline L1 was obtained in good yield (70%) by crystallization from CH2Cl2. The successful synthesis of L1 was verified by NMR analysis, mass spectrometry, and single-crystal XRD diffraction studies (Fig. 1). The <sup>11</sup>B NMR resonance of L1 was located at  $\delta$  22.8 ppm and is similar to that observed for three-coordinate boron in other TBDPhos ligands and complexes, such as those described here. A sharp  $^{31}$ P NMR chemical shift was observed at  $\delta$  164.5 ppm.

Once <sup>Cl</sup>TBDPhos was isolated, it was used to prepare the phosphoramidite ligands <sup>iPrO</sup>TBDPhos (**L2**) and <sup>F-iPrO</sup>TBDPhos (**L3**) with bulky  $OC_3H_7$  and  $OC_3HF_6$  substituents, respectively. Both ligands were prepared by addition of four equivalents of the respective alcohol (2-propanol or 1,1,1,3,3,3-hexafluoro-2-propanol) to stirring solutions of <sup>Cl</sup>TBDPhos in the presence of four equivalents of NEt<sub>3</sub>. After workup, the ligands were isolated in good yields of 74% (**L2**) and 89% (**L3**). The <sup>11</sup>B NMR resonance observed for **L2** at  $\delta$  24.8 ppm was shifted 2 ppm

Scheme 1. Comparison of the synthesis of MeOTBDPhos described previously [29] and alkoxy-substituted TBDPhos ligands L2 and L3 via precursor ClTBDPhos (L1).

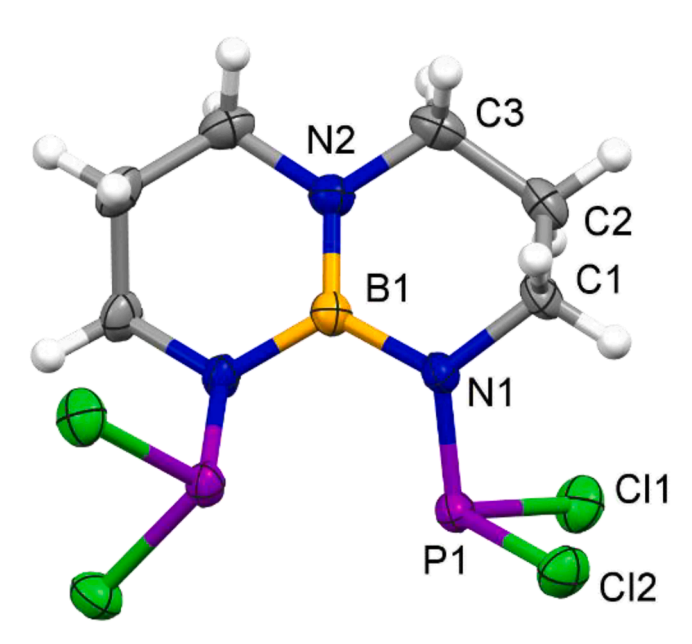


**Fig. 1.** Molecular structure of <sup>Cl</sup>TBDPhos (**L1**) with thermal ellipsoids shown at the 50% probability level. Select bond distances: P1-Cl1 = 2.0898(6) Å, P1-Cl2 = 2.0746(6) Å, P1-N1 = 1.656(1) Å, P1-N1 = 1.466(2) Å, P1-N2 = 1.395(3) Å.

downfield compared to **L1**, and the <sup>31</sup>P NMR resonance was located at  $\delta$  139.1 ppm (Table 2). The <sup>11</sup>B NMR resonance of **L3** was similar to **L2** at  $\delta$  24.2 ppm, but the <sup>31</sup>P NMR resonance was located more downfield at  $\delta$  152.9 ppm due to the electron withdrawing fluorine substituents. The <sup>19</sup>F NMR spectrum for **L3** revealed two multiplets at  $\delta$  –74.3 ppm and –74.5 ppm indicating slight asymmetry of the fluorinated substituents (Table 2).

#### 3.2. Synthesis and characterization of metal complexes

To establish the coordination chemistry of **L2** and **L3**, we synthesized the square planar nickel, palladium and platinum complexes shown in Scheme 2. The chloride complexes  $\mathbf{2} - \mathbf{6}$  were prepared by treating (DME)NiCl<sub>2</sub> (DME = 1,2-dimethoxyethane) (PhCN)<sub>2</sub>PdCl<sub>2</sub>, or (COD) PtCl<sub>2</sub> (COD = 1,5-cyclooctadiene) with **L2** or **L3** in CH<sub>2</sub>Cl<sub>2</sub> and isolated in good crystalline yields after workup (52–77%). (MeOTBDPhos)PdCl<sub>2</sub> (1) has yet to be reported and was prepared for comparison to  $\mathbf{2} - \mathbf{6}$  and (MeOTBDPhos)PtCl<sub>2</sub> published previously [29]. NMR analysis of all five complexes revealed <sup>11</sup>B NMR resonances with similar chemical shifts in the range of  $\delta$  21.4 – 22.3 ppm. The <sup>31</sup>P NMR resonances for  $\mathbf{1} - \mathbf{6}$ 

Table 2

 $^{11}\text{B},\,^{19}\text{F}$  and  $^{31}\text{P}$  NMR resonances and Pt-P coupling constants in CDCl $_3$ . Chemical shifts are reported in  $\delta$  units relative to BF $_3$ :Et $_2\text{O}$  ( $^{11}\text{B};\,\delta$ 0.0 ppm), 0.05%  $C_6H_5\text{CF}_3$  in  $C_6D_6$  ( $^{19}\text{F};\,\delta$ –62.9 ppm), and 85%  $H_3\text{PO}_4$  ( $^{31}\text{P};\,\delta$ 0.0 ppm). Resonances and shifts reported previously for  $^{\text{MeO}}\text{TBDPhos}$  and its complexes with Pt are shown for comparison.

Compound	<sup>11</sup> B (FWHM in Hz) <sup>a</sup>	<sup>19</sup> F{ <sup>1</sup> H}	<sup>31</sup> P { <sup>1</sup> H}	<sup>1</sup> J <sub>PtP</sub> (Hz)
ClTBDPhos (L1)b	22.8 (150)	_	164.5	
MeOTBDPhos <sup>c</sup>	24.7 (220)	_	145.6	_
iPrOTBDPhos (L2)	24.8 (440)	_	139.1	_
F-iPrOTBDPhos (L3)	24.2 (300)	-74.3,	152.1	_
		-74.5		
(MeOTBDPhos)PdCl <sub>2</sub> (1)	22.8 (310)		96.2	
(MeOTBDPhos)PtCl <sub>2</sub> <sup>c</sup>	22.7 (260)	_	69.9	4895
$(^{\mathrm{iPrO}}\mathrm{TBDPhos})\mathrm{PdCl}_{2}$ (2)	22.0 (380)	_	87.6	-
(iPrOTBDPhos)PtCl <sub>2</sub> (3)	22.3 (350)	_	60.7	4882
(F-iPrOTBDPhos)NiCl <sub>2</sub> (4)	21.4 (400)	-72.9,	98.1	-
		-74.2		
(F-iPrOTBDPhos)PdCl <sub>2</sub> (5)	21.6 (400)	-73.0,	96.5	-
		-74.0		
(F-iPrOTBDPhos)PtCl <sub>2</sub> (6)	21.8 (250)	-73.1,	69.6	4895
		-73.9		
(MeOTBDPhos)Pt	23.2 (410)	-	97.7	3918
$(S_2C_6H_4)^c$				
$(^{iPrO}TBDPhos)Pt(S_2C_6H_4)$	22.5 (480)	-	89.7	3895
(7)				
$(^{F-irO}TBDPhos)Pt(S_2C_6H_4)$	22.2 (340)	-72.6,	102.6	3852
(8)		-72.7		

<sup>&</sup>lt;sup>a</sup> FWHM = full width at half maximum.

showed clear periodic trends based on the identity of the group 10 metal. For example, the  $^{31}P$  resonances for the  $(^{F-iPrO}\text{TBDPhos})\text{MCl}_2$  complexes shifted from  $\delta$  98.1 to 96.5 to 69.6 ppm for M = Ni, Pd, and Pt respectively. Similar results were observed for  $(^{iPrO}\text{TBDPhos})\text{MCl}_2$  with M = Pd or Pt (Table 2). In addition to their chemical shifts, the  $^{31}P$  NMR data for the Pt complexes 3 and 6 revealed  $^{195}\text{Pt}^{-31}P$  satellite peaks with coupling constants of  $^{1}J_{Pt-P}=4882$  Hz and 4895 Hz, respectively, similar to that reported for ( $^{\text{MeO}}\text{TBDPhos})\text{PtCl}_2$ . As observed for free L3, two  $^{19}F$  NMR multiplet resonances were observed for 4 - 6 between  $\delta$  -72.9 and -74.2 ppm.

We have shown previously that the chloride ligands are often displaced under conditions used to investigate ligand-centered reactivity in TBDPhos complexes, which makes it challenging to isolate and study the influence of different ligand modifications on reactivity because multiple complexes may be present in solution. We have shown that this issue can be addressed by swapping out the chloride ligands with more

<sup>&</sup>lt;sup>b</sup> Collected in C<sub>6</sub>D<sub>6</sub>.

c Reference [29].

$$(RO)_{2}P P (OR)_{2} \xrightarrow{(L)MCl_{2}} (RO)_{2}P P (OR)_{2} \xrightarrow{(RO)_{2}P P (OR)_{2}} (RO)_{2}P P (OR)_{2} \xrightarrow{(RO)_{2}P P (OR)_{2}} (RO)_{2}P P (OR)_{2}$$

$$R = {}^{i}Pr (L2) \text{ or } C_{3}HF_{6} (L3)$$

$$L = DME (M = Ni), 2 PhCN (M = Pd), COD (M = Pt)$$

Scheme 2. Synthesis of diphosphoramidite complexes with chloride (1-6) and dithiolate ancillary ligands (7 and 8).

chelating and more strongly binding ligands such as 1,2-benzenedithiolate [29], and here we have prepared ( $^{iPrO}$ TBDPhos)Pt( $S_2C_6H_4$ ) (7) and ( $^{F-iPrO}$ TBDPhos)Pt( $S_2C_6H_4$ ) (8) for comparison.

Treating **3** and **6** with 1,2-benzenedithiol and two equiv. of NEt<sub>3</sub> in CH<sub>2</sub>Cl<sub>2</sub> yielded **7** and **8**. These complexes were isolated in 81% and 40% crystalline yield, respectively, after workup. The  $^{11}B$  NMR resonances for **7** and **8** showed no significant change when compared to their parent chloride complexes **3** and **6**. As expected, the  $^{31}P$  NMR data revealed more upfield chemical shifts at  $\delta$  89.7 ppm ( $^{1}J_{PtP}=3895$  Hz) and  $\delta$  102.6 ppm ( $^{1}J_{PtP}=3852$  Hz) and are similar to those reported previously for ( $^{MeO}TBDPhos)Pt(S_{2}C_{6}H_{4})$  at  $\delta$  97.7 ppm ( $^{1}J_{PtP}=3918$  Hz). All three dithiolate complexes show a decrease of a  $\sim$ 1000 Hz in the  $^{195}Pt\cdot^{31}P$  coupling constant compared to their chloride complexes. It has been shown that the  $^{195}Pt\cdot^{31}P$  coupling constants correlate well to Pt-P bond length [46], and XRD studies show how the Pt-P bond distances increase in **7** and **8** in response to the stronger trans influence of the dithiolate ligand compared to chloride.

#### 3.3. Molecular structures of metal complexes

Single-crystal XRD data were collected on the chloride complexes 1, 2, 3, and 5 and the dithiolate complexes 7 and 8 for comparison to previously reported platinum complexes with  $^{\rm MeO}$ TBDPhos. As expected, all six complexes are rigorously square planar (Figs. 2 and 3), and selected distances and angles are compiled in Table 3 alongside known  $^{\rm MeO}$ TBDPhos derivatives with the same ancillary ligands.

Comparison of the ( $^{RO}$ TBDPhos)MCl $_2$  complexes reveals significant changes in the P-M-P bite angles, which decrease in response to

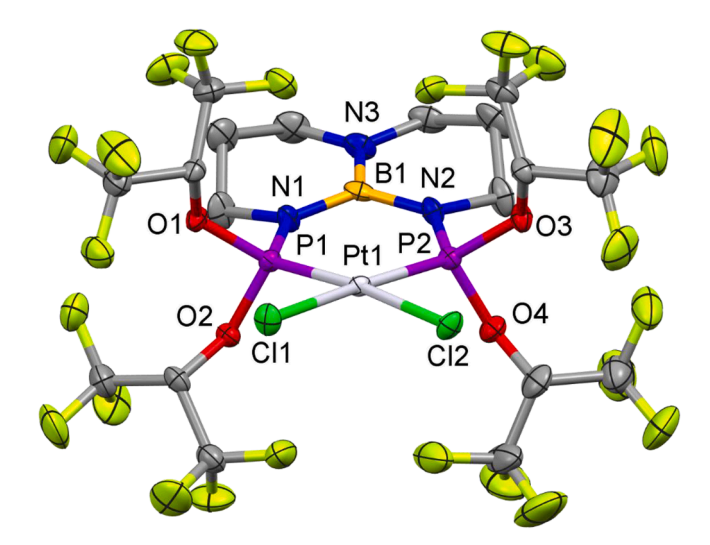


**Fig. 2.** Molecular structure of **6** with thermal ellipsoids shown at the 50% probability level. Only one of the two molecules in the asymmetric unit are shown. Hydrogen atoms were omitted for easier viewing of the local coordination environment around Pt.

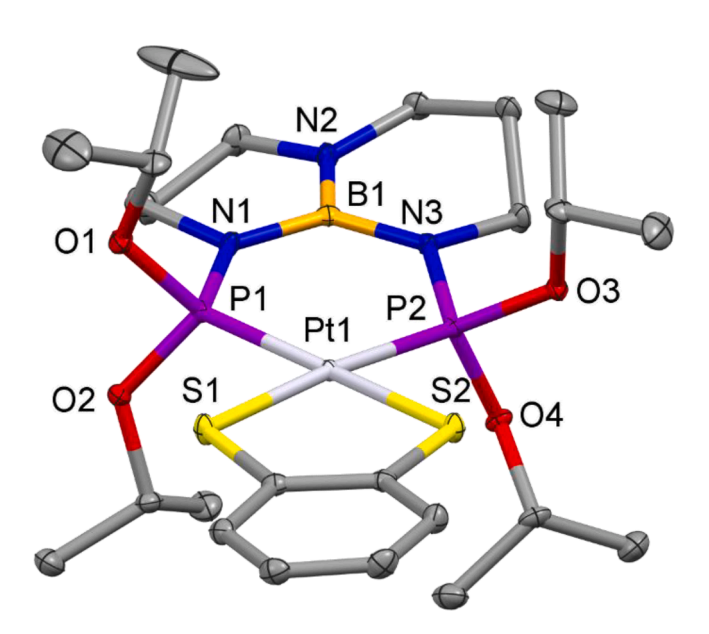


**Fig. 3.** Molecular structure of **7** with thermal ellipsoids shown at the 50% probability level. Hydrogen atoms were omitted for easier viewing of the local coordination environment around Pt.

increasing steric bulk on the phosphorus substituents from 97.47(3)° in (MeOTBDPhos)PtCl<sub>2</sub> to 96.17(4)° in (iPrOTBDPhos)PtCl<sub>2</sub> (3) to 93.98(4)° in (F-iPrOTBDPhos)PtCl<sub>2</sub> (6); similar differences are observed in the Pd complexes 1 and 2 (Table 3). In contrast to the differences in bite angle, only subtle changes are observed in the M-P and M-Cl bond distances. However, the Pt-P bond distances increase by 0.02 - 0.03 Å upon swapping the chloride ligands for 1,2-benzenedithiolate, consistent with the decrease in <sup>195</sup>Pt-<sup>31</sup>P coupling constants shown in Table 2. The Pt-P distances in the ( $^{RO}$ TBDPhos)Pt( $S_2C_6H_4$ ) complexes range from 2.206(2) to 2.2246(5) Å, which are 0.03 - 0.14 Å shorter compared to those reported in Pt diphosphine complexes with 1,2-aryldithiolates [47-50]. Likewise, the Pt-S bonds in the (ROTBDPhos)Pt(S<sub>2</sub>C<sub>6</sub>H<sub>4</sub>) complexes are slightly longer when compared to the same set of reported diphosphine complexes. The decreased Pt-P and increased Pt-S distances in (ROTBDPhos)Pt(S<sub>2</sub>C<sub>6</sub>H<sub>4</sub>) complexes compared to diphosphines likely reflects the increased  $\pi$ -acidity and trans influence of the diphosphoramidite ligands.

As a final comparison, we can evaluate the influence of fluorinated (F-iPrO) and non-fluorinated (MeO and iPrO) substituents on bond distances in the ligands themselves. Perhaps unsurprisingly, the  $^{\text{MeO}}$ TBPhos and  $^{\text{iPrO}}$ TBDPhos complexes show only subtle differences in ligand bond distances ( $\leq\!0.01$  Å) when the identity of the ancillary ligand is the same. However, substituting these non-fluorinated substituents for OC<sub>3</sub>HF<sub>6</sub> causes the P-O bonds to increase by 0.02 – 0.03 Å and the P-N distances to decrease by 0.03 – 0.04 Å in  $^{\text{F-iPrO}}$ TBDPhos complexes. The fluorinated substituents also cause subtle changes in the

J.D. Culpepper et al. Polyhedron 221 (2022) 115877

Table 3
Selected bond distances (Å) and angles (°) from single-crystal XRD data for alkoxy-substituted TBDPhos complexes with palladium and platinum.

	( <sup>R</sup> TBDPhos)PdCl <sub>2</sub>		$(^{ m R}{ m TBDPhos}){ m PtCl}_2$		(RTBDPhos)Pt(S <sub>2</sub> C <sub>6</sub> H <sub>4</sub> )			
	R = OMe (1)	$R = O^{i}Pr(2)$	$R = OMe^{29}$	$R = O^i Pr (3)$	$R = OC_3HF_6 (6)^a$	$R = OMe^{29}$	$R = O^{i}Pr (7)$	$R = OC_3HF_6 (8)$
M-P	2.2023(7)	2.2122(4)	2.1925(6)	2.201(1)	2.187(1)	2.206(2)	2.2246(5)	2.214(1)
	_	2.2093(5)	_	2.194(1)	2.1928(9)	2.218(2)	2.2228(6)	2.218(1)
B-N	1.401(6)	1.416(2)	1.409(5)	1.400(6)	1.397(5)	1.410(9)	1.419(3)	1.393(7)
B-N(P)	1.453(3)	1.456(2)	1.457(3)	1.449(6)	1.463(5)	1.451(9)	1.455(2)	1.471(7)
	_	1.453(2)	_	1.460(6)	1.474(5)	1.459(8)	1.463(3)	1.475(7)
P-N	1.646(2)	1.652(1)	1.649(2)	1.658(4)	1.625(3)	1.654(5)	1.663(2)	1.618(4)
	_	1.653(1)	_	1.653(4)	1.624(3)	1.647(5)	1.661(2)	1.624(4)
P-O	1.581(2)	1.582(1)	1.581(2)	1.581(3)	1.613(3)	1.588(5)	1.593(1)	1.616(4)
	1.585(2)	1.588(1)	1.586(2)	1.593(3)	1.617(2)	1.592(5)	1.593(1)	1.623(4)
	_	1.579(1)	1.581(2)	1.584(3)	1.608(3)	1.586(5)	1.599(1)	1.622(4)
	_	1.591(1)	1.586(2)	1.588(3)	1.602(3)	1.600(5)	1.595(1)	1.627(4)
M-L <sup>b</sup>	2.3500(7)	2.3589(5)	2.3573(6)	2.359(1)	2.3474(9)	2.317(2)	2.3212(6)	2.310(1)
	_	2.3566(5)		2.353(1)	2.341(1)	2.320(2)	2.3260(5)	2.312(1)
P-M-P	96.35(4)	95.83(2)	97.47(3)	96.17(4)	93.98(4)	94.04(6)	94.98(2)	93.43(5)
L-M-L	91.44(4)	89.31(2)	89.16(3)	87.31(4)	87.42(3)	88.57(5)	88.15(2)	87.76(4)
Σ ΝΒΝ	360.0(5)	360.0(2)	360.0(2)	360.0(7)	359.9(6)	359.9(6)	360.1(3)	360.0(8)

<sup>&</sup>lt;sup>a</sup> Values shown for one of two molecules in asymmetric unit.

B-N bonds in the TBD backbone. The B-N(P) and B-N bonds in the F-iPrOTBDPhos complexes **6** and **8** are among the longest and shortest observed in TBDPhos complexes to date. These findings appear to correlate with qualitative observations suggesting that F-iPrOTBDPhos are more reactive than identical complexes with MeOTBDPhos and iPrOTBDPhos. Studies are currently underway to quantify these substituent-induced reactivity differences more rigorously in these and related TBDPhos complexes.

#### 4. Conclusions

In summary, we have described a convenient and modular method to prepare diphosphoramidite ligands derived from TBD. New alkoxy-substituted TBDPhos ligands were prepared in good yields by treating the precursor ClTBDPhos (L1) with dry alcohols. This avoids the need for ClP(OR)<sub>2</sub> starting materials that can be more difficult to prepare and purify. We demonstrated how this method could be used to prepare two new TBDPhos ligands with and without fluorinated substituents (L2 and L3), and we compared the structures and spectroscopic properties of their complexes with group 10 metals. Side-by-side comparisons with MeOTBDPhos complexes containing ancillary chloride and 1,2-benzene-dithiolate ligands showed how electronic and steric properties of the alkoxy substituents at phosphorus give rise to structural differences around the metal and in the ligand itself. Reactivity studies are currently in progress to determine how these changes affect ligand-centered reactions at the TBD backbone.

#### **Declaration of Competing Interest**

The authors declare that they have no known competing financial interests or personal relationships that could have appeared to influence the work reported in this paper.

#### Acknowledgment

We thank Dale Swenson for collecting the single-crystal XRD data.

## Funding

This work was generously supported by the National Science Foundation (CHE-1650894), the National Science Foundation Graduate Research Fellowship under Grant No. 000390183 (J. D. C.), and American Chemical Society's Petroleum Research Fund (62151-ND3). The National Science Foundation is also gratefully acknowledged for

supporting the purchase of a new X-ray diffractometer under award CHE-1828117.

#### Appendix A. Supplementary data

NMR spectra. CCDC 2157714-2157720 contains the supplementary crystallographic data for  $\bf L1, 1-3$ , and  $\bf 6-8$ . These data can be obtained free of charge via http://www.ccdc.cam.ac.uk/conts/retrieving.html, or from the Cambridge Crystallographic Data Centre, 12 Union Road, Cambridge CB2 1EZ, UK; fax: (+44) 1223-336-033; or e-mail: deposit@ccdc.cam.ac.uk. Supplementary data to this article can be found online at https://doi.org/10.1016/j.poly.2022.115877.

#### References

- [1] U. Pradere, E.C. Garnier-Amblard, S.J. Coats, F. Amblard, R.F. Schinazi, Chem. Rev. 114 (2014) 9154–9218.
- [2] S.L. Beaucage, R.P. Iyer, Tetrahedron 49 (1993) 6123-6194.
- [3] S.L. Beaucage, R.P. Iyer, Tetrahedron 49 (1993) 1925–1963.
- [4] S.L. Beaucage, M.H. Caruthers, Curr. Protoc. Nucleic Acid Chem. (2001). Chapter 3, Unit 33.
- [5] R.A. Hughes, A.D. Ellington, Cold Spring Harbor Perspect. Biol. 9 (2017) a023812/ 023811-a023812/023818.
- [6] G. De Crozals, C. Farre, M. Sigaud, P. Fortgang, C. Sanglar, C. Chaix, Chem. Commun. 51 (2015) 4458–4461.
- [7] A.F. Sandahl, T.J.D. Nguyen, R.A. Hansen, M.B. Johansen, T. Skrydstrup, K. V. Gothelf, Nat. Commun. 12 (2021) 2760.
- [8] P.C. Kamer, P.W. van Leeuwen, Phosphorus (III) Ligands in Homogeneous Catalysis: Design and Synthesis, John Wiley & Sons, 2012.
- [9] B.L. Feringa, Acc. Chem. Res. 33 (2000) 346–353.
- [10] J.G. de Vries, L. Lefort, Chem. Eur. J. 12 (2006) 4722–4734.
- [11] A.J. Minnaard, B.L. Feringa, L. Lefort, J.G. de Vries, Acc. Chem. Res. 40 (2007) 1267–1277.
- [12] L. Eberhardt, D. Armspach, J. Harrowfield, D. Matt, Chem. Soc. Rev. 37 (2008) 839–864.
- [13] J.-H. Xie, Q.-L. Zhou, Acc. Chem. Res. 41 (2008) 581-593.
- [14] J.F. Teichert, F.B.L. Angew, Chem. Int. Ed. 49 (2010) 2486–2528.
- [15] R.K. Friedman, K.M. Oberg, D.M. Dalton, T. Rovis, Pure Appl. Chem. 82 (2010) 1353–1364.
- [16] P. Tosatti, A. Nelson, S.P. Marsden, Org. Biomol. Chem. 10 (2012) 3147–3163.
- [17] J. Wassenaar, J.N.H. Reek, Org. Biomol. Chem. 9 (2011) 1704–1713.
- [18] H.W. Lam, Synthesis (2011) 2011–2043.
- [19] J. Pedroni, N. Cramer, Chem. Commun. 51 (2015) 17647–17657.
- [20] X.-S. Chen, C.-J. Hou, X.-P. Hu, Synth. Commun. 46 (2016) 917–941.
- [21] S.L. Rossler, D.A. Petrone, E.M. Carreira, Acc. Chem. Res. 52 (2019) 2657–2672.
   [22] M.T. Reetz, G. Mehler, O. Bondarev, Chem. Commun. (2006) 2292–2294.
- [23] L. Eberhardt, D. Armspach, D. Matt, B. Oswald, L. Toupet, Org. Biomol. Chem. 5
- (2007) 3340–3346.
  [24] K.N. Gavrilov, A.A. Shiryaev, I.V. Chuchelkin, S.V. Zheglov, E.A. Rastorguev, V.
- [24] K.N. Gavriiov, A.A. Sniryaev, I.V. Chucheikin, S.V. Znegiov, E.A. Rastorguev, V. A. Davankov, A. Borner, Tetrahedron Asymmetry 23 (2012) 1052–1057.
- [25] D. Drommi, G. Micalizzi, C.G. Arena, Appl. Organomet. Chem. 28 (2014) 614-619.
- [26] D. Drommi, A.C.G. Appl, Organomet. Chem. 31 (2017) n/a.

 $<sup>^{</sup>b}$  L = Cl or S.

- [27] Y. Luo, G. Ouyang, Y. Tang, Y.-M. He, Q.-H. Fan, J. Org. Chem. 85 (2020) 8176–8184
- [28] T. Shirai, Yamamoto, Y. Synthesis 2021, Ahead of Print. https://doi.org/10.1055/a-1683-9455.
- [29] K. Lee, J.D. Culpepper, R. Parveen, D.C. Swenson, B. Vlaisavljevich, S.R. Daly, Organometallics 39 (2020) 2526–2533.
- [30] K. Lee, C.M. Donahue, S.R. Daly, Dalton Trans. 46 (2017) 9394-9406.
- [31] K. Lee, C. Kirkvold, B. Vlaisavljevich, S.R. Daly, Inorg. Chem. 57 (2018) 13188–13200.
- [32] K. Lee, A.V. Blake, C.M. Donahue, K.D. Spielvogel, B.J. Bellott, D.S.R. Angew, Chem. Int. Ed. 58 (2019) 12451–12455.
- [33] K. Lee, C.W. Kim, J.L. Buckley, B. Vlaisavljevich, S.R. Daly, Dalton Trans. 48 (2019) 3777–3785.
- [34] K. Lee, P.-N. Lai, R. Parveen, C.M. Donahue, M.M. Wymore, B.A. Massman, B. Vlaisavljevich, T.S. Teets, S.R. Daly, Chem. Commun. 56 (2020) 9110–9113.
- [35] P. Fritz, K. Niedenzu, J.W. Dawson, Inorg. Chem. 4 (1965) 886–889.
- [36] E.F. Rothgery, K. Niedenzu, Syn. Inorg. Metal-Org. Chem. 1 (1971) 117–121.
- [37] Bruker Bruker AXS Inc., Madison, WI, USA 2001.
- [38] G.M. Sheldrick, Acta Crystallogr., Sect. A Found. Adv. 2015, 71, 3-8.
- [39] G.M. Sheldrick, Acta Crystallogr., Sect. C Struct. Chem. 71 (2015) 3-8.

- [40] O.V. Dolomanov, L.J. Bourhis, R.J. Gildea, J.A.K. Howard, H. Puschmann, J. Appl. Crystallogr. 42 (2009) 339–341.
- [41] C.F. Macrae, P.R. Edgington, P. McCabe, E. Pidcock, G.P. Shields, R. Taylor, M. Towler, J. van de Streek, J. Appl. Crystallogr. 39 (2006) 453–457.
- [42] J. Chatt, W. Hussain, G.J. Leigh, H.M. Ali, C.J. Pickett, D.A.J. Rankin, Chem. Dalton Trans Soc. (1985) 1131–1136.
- [43] L. Manojlovic-Muir, I.R. Jobe, B.J. Maya, R.J.J. Puddephatt, Chem. Dalton Trans Soc. (1987) 2117–2124.
- [44] Y. Xu, H. Wei, J. Xia, Liebigs Ann. Chem. (1988) 1139-1143.
- [45] M.C. Nielsen, K.J. Bonney, F. Schoenebeck, Angew. Chem., Int. Ed. 53 (2014) 5903–5906.
- [46] P.G. Waddell, A.M.Z. Slawin, J.D. Woollins, Dalton Trans. 39 (2010) 8620-8625.
- [47] L.L. Maisela, A.M. Crouch, J. Darkwa, I.A. Guzei, Polyhedron 20 (2001) 3189–3200.
- [48] A. Nova, R. Mas-Balleste, G. Ujaque, P. Gonzalez-Duarte, A. Lledos, Dalton Trans. (2009) 5980–5988.
- [49] M.J.G. Lesley, W. Clegg, T.B. Marder, N.C. Norman, A.G. Orpen, Scott, A. J. Starbuck, J. Acta Crystallogr., Sect. C Cryst. Struct. Commun. C55 (1999) 1272–1275.
- [50] J.D. Wrixon, J.J. Hayward, O. Raza, J.M. Rawson, Dalton Trans. 43 (2014) 2134–2139.